

Tug-of-war of molecular motors: the effects of uneven load sharing

Sebastián Bouzat¹ and Fernando Falo²

¹ Consejo Nacional de Investigaciones Científicas y Técnicas, Centro Atómico Bariloche (CNEA), (8400) Bariloche, Argentina.

² Dpto de Física de la Materia Condensada and BIFI, Universidad de Zaragoza, 50009 Zaragoza, Spain.

E-mail: bouzat@cab.cnea.gov.ar

Abstract. We analyze theoretically the problem of cargo transport along microtubules by motors of two species with opposite polarities. We consider two different one-dimensional models previously developed in the literature. On the one hand, a quite widespread model which assumes equal force sharing, here referred to as mean field model (MFM). On the other hand, a stochastic model (SM) which considers individual motor-cargo links. We find that in generic situations the MFM predicts larger cargo mean velocity, smaller mean run time and less frequent reversions than the SM. These phenomena are found to be consequences of the load sharing assumptions and can be interpreted in terms the probabilities of the different motility states. We also explore the influence of the viscosity in both models and the role of the stiffness of the motor-cargo links within the SM. Our results show that the mean cargo velocity is independent of the stiffness while the mean run time decreases with such a parameter. We explore the case of symmetric forward and backward motors considering kinesin-1 parameters, and the problem of transport by kinesin-1 and cytoplasmic dyneins considering two different sets of parameters previously proposed for dyneins.

PACS numbers: 87.16.A, 87.16.Nn, 87.16.Uv

Keywords: molecular motors, tug of war, load sharing

Submitted to: *Phys. Biol.*

1. Introduction

Transport of cargo driven by multiple molecular motors along microtubules has become a very active subject of research because of its relevance for many cellular functions [1, 2, 3, 4]. In recent years, a myriad of experiments and models have attempted to understand the way in which motors work together [4, 5, 6, 7, 8, 9], and, still, there are many fundamental details which remain unclear and deserve further research, most particularly for the case of bidirectional transport by two motor species.

The complexity of the multiple motor systems and the difficulties for controlling the experiments are often quite important so that performing the connection between models and experiments must be done carefully. Models involve always many parameters, including for instance detachment and attachment rates, stall forces, motor stiffness and viscosity of the media. Usually, many of these parameters are a priori not well known in the experiments, and even more fundamental features such as the number of motors, or whether more than a single species is participating on the transport, remain unclear. Thus, distinct models may provide different fitting of the experimental data and, consequently, different interpretations. Moreover, recent *in vivo* experiments [10] have revealed important differences with *in vitro* systems. In this context, a detailed knowledge of the consequences of specific modeling assumptions as well as the comparison of different kinds of models becomes quite relevant. The aim of this paper is to contribute in these two important aspects.

References [11] and [12] have originated a modeling framework that has largely contributed to the understanding of transport by several motors. The model introduced in [11] deals with cargo transport by a single class of motors, while in [12] the formalism is extended to account for bidirectional transport associated to tug of war between two motor types with opposite polarities. Assuming certain force–velocity relations, and specific attachment and detachment probabilities for individual motors, the model enables the calculation of the probabilities of different motility states characterized by different number of motors, and the reproduction of trajectories and velocity distributions as well. In a series of papers [7, 13, 14, 15] the model was further developed and several effects and transport conditions have been analyzed, providing a deep physical insight on the problem. An important assumption of the model is that all the motors of the same polarity simultaneously engaged to the microtubule share equally the load. In real systems, however, fluctuations of the distances between motor-microtubule binding position and motor-cargo binding position may lead to non-negligible differences between the forces supported by the different motors [8, 16, 17, 18]. Consequently, the model would eventually fail to predict exact quantitative results. In reference [17], the model was referred to as *mean field* due to the equal sharing of load approximation. We will keep such a name throughout this work.

Several models have gone beyond the mean field approach by considering independent motor-cargo links for each motor, and incorporating different degree of detail in their description of individual motor properties [8, 9, 17, 19, 20]. Although

such models generally provide less instrumental (and less elegant) formulations than the mean field model, and they mostly lack analytical results, they may be more successful in predicting numerical results for multiple motors through simulations based on individual motor parameters. In a different but related context, models in references [21] and [22] consider the load applied only to the leading motor and constitute thus interesting extreme examples of models beyond mean field. Although not directly connected to our approach for processive motors on microtubules, studies on non-processive motors [23, 24] and general ratchet models [25] provide also relevant analysis of bidirectional motion in many motor systems.

In this paper we investigate bidirectional cargo transport by two opposing teams of processive motors within two different models. On the one hand, the mean field model. On the other hand, a recently introduced [19] stochastic model which considers independent cargo-motor links for individual motors, allowing for uneven load sharing. In this way, at the same time that we investigate how cargo transport depends on the system parameters, we are able to clearly identify the consequences of the assumption of equal load sharing. Our work follows the spirit of the paper by Kunwar and Mogilner [17]. There, the authors compared results from both kind of models focussing on the case of cargo transport by a single team of motors, and provided also an analysis of the velocity distributions for bidirectional transport. Moreover, they studied the influence of the non linearities of the force-velocity relations of individual motors.

Our studies focus on analyzing the dependence of cargo transport on the number of motors of each polarity, the viscous drag, and the stiffness of the motor cargo link, while we do not consider the influence of additional load forces acting on cargo. In Section 2 we present the models. Section 3 studies the case of equal forward and backward motors. The effects of varying the number of motors to each side and the influence of viscous drag are analyzed within both models. In section 4 we present results for bidirectional transport by asymmetric motors considering system parameters compatible with kinesin-1 and cytoplasmic dynein. Section 5 is devoted to the conclusions.

2. Models and methods

As indicated in the introduction, we will consider two different models for the analysis of cargo transport by multiple motors. The mean field model (MFM), and our recently proposed stochastic model (SM). We first introduce the characteristics that are common to both.

The two models consider the cargo as a point particle which performs a continuous trajectory $x(t)$ in one dimension. The cargo is linked to N_f forward motors and N_b backward motors. The first of them can pull the cargo in the positive direction while the second can pull it in the negative one. At a given time, the number of forward and backward motors engaged to the microtubule are respectively $n_f(t) \leq N_f$ and $n_b(t) \leq N_b$. Each engaged motor i , detaches from the microtubule with a probability per time unit given by $\epsilon \exp(-|f_i|/F_d)$. Here f_i is the instantaneous force exerted by motor i

on the cargo, ϵ is the reference zero-load detachment rate and $F_d > 0$ is the detachment force. We will call $\epsilon_f, \epsilon_b, F_{df}$ and F_{db} the corresponding parameters for forward and backward motors. Conversely, a detached motor engages to the microtubule with rate Π_f or Π_b , according to its type.

When loaded with a force $f_i > 0$ (considered positive if exerted against the polarity of the motor), the motor i advances with velocity

$$v_i = \begin{cases} v_0(1 - f_i/F_s) & \text{for } f_i \leq F_s \\ v_1(1 - f_i/F_s) & \text{for } f_i > F_s. \end{cases} \quad (1)$$

Here $F_s > 0$ is the stall force, v_0 the zero-load velocity and v_1 a reference backward velocity. Considering both motor species we have the system parameters $F_{sf}, F_{sb}, v_{0f}, v_{0b}, v_{1f}$ and v_{1b} . The linear force-velocity relation for single motors of Eq. (1) is a natural choice for comparing the SM and MFM since it is used in most works on the MFM [7, 12, 13] and is also a common assumption in other theoretical models [17, 26, 27]. Studies in [17] suggest that the consideration of a general non-linear relations would lead to no relevant qualitative changes in the results. It is important to mention that, while Eq.(1) is taken as instantaneously exact in the MFM, within the SM it is only valid in terms of time averages, i.e. v_i is the mean velocity of a motor subject to a constant force f_i .

The way to compute the forces f_i and the cargo motion depends on the model as we explain in the following subsections.

2.1. Cargo dynamics in the mean field model

The MFM [12] assumes that all the motors (backward and forward) move with the same velocity than cargo at any time, and that motors of the same polarity share the force equally. It also assumes the total force acting on the cargo vanishes at almost any time (it has discontinuities at the times at which the number of engaged motors changes). With such hypothesis, by performing a force balance and using the force-velocity relation for single motors of Eq.(1), it is possible to obtain the cargo velocity as a function of the numbers of engaged motors n_f and n_b [12]. We thus have a discrete set of allowed cargo velocities $v(n_f, n_b)$, corresponding to the different motility states (n_f, n_b) considering $n_f = 0, 1, \dots, N_f$, $n_b = 0, 1, \dots, N_b$. The model can be implemented through two main different methods. First, by means of a master equation which allows to compute stationary probabilities $P(n_f, n_b)$ and, thus, velocity distributions $P(v)$. And, second, by means of a Gillespie algorithm [12, 28] which allows to compute cargo trajectories. This latter numerical scheme determines the temporal evolution of the system by ruling the transitions between different motility states taking into account the attachment and detachment probabilities. During each time interval between two transitions, the cargo velocity is assumed to be constant and equal to the corresponding value $v(n_f, n_b)$.

For two motors species, the model was first introduced in [12] without considering any external force. Then, in [15] it was generalized to include the cases of viscous

environments and non vanishing load forces. This is done by modifying appropriately the force balance, but without changing any of the model hypothesis mentioned before.

As part of our studies we have implemented both the master equation and Gillespie formulations of the model without external forces (although we will only show results from the latter), and also the Gillespie method considering non negligible viscous drag. We have checked that our results correctly reproduce some selected ones from references [12] and [15]. In all cases we have assumed the linear force-velocity profile of Eq.(1).

2.2. Stochastic model

As other models in the literature [8, 17], the stochastic model introduced in [19] considers a Langevin dynamics for cargo motion, a discrete-steps stochastic dynamics for individual motors and cargo-motor links described by non-linear springs. The Langevin equation for cargo is

$$\gamma \dot{x}_c = \sum_i f_i + \xi(t). \quad (2)$$

Here γ is the viscous drag, f_i ($i = 1, \dots, N = N_f + N_b$) the force exerted by the i -th motor and $\xi(t)$ the white thermal noise. The viscous drag is defined through the Stokes relation $\gamma = 6\pi\eta r$ [8, 17], where η is the viscosity of the medium and r the radius of the cargo for which we consider $r = 500nm$ throughout the paper. The thermal noise satisfies $\langle \xi(t) \rangle = 0$ and the correlation formula $\langle \xi(t_1)\xi(t_2) \rangle = 2D\delta(t_1 - t_2)$ [29]. Here $\langle \rangle$ represents ensemble average, $\delta(t)$ is the Dirac Delta and D the diffusion coefficient satisfying the fluctuation-dissipation relation $D = k_B T / \gamma$ [29], with k_B the Boltzmann constant and T the temperature. In all our calculations we consider $T = 300K$.

Each motor is modeled as a particle that can occupy discrete positions separated by $\Delta x = 8nm$ along the same spatial coordinate used for the cargo. Its dynamics is governed by a Monte Carlo algorithm [19] that rules the elementary processes of step forward, step back, detachment, and attachment. At each time step of duration dt , an engaged forward motor has a probability $p_{jump} = dt/\tau_D(F)$ of performing an $8nm$ step, which may be forward (right) with probability $P_r(F) = [R(F)/(1 + R(F))]$ or backward (left) with probability $P_l(F) = [1/(1 + R(F))]$. Here $\tau_D(F)$ is the dwell time [30, 31] and $R(F)$ is the forward-backward ratio of jumps [30, 31, 32]. The resulting mean velocity for a single forward motor with constant load F is $v(F) = \Delta x(P_r(F) - P_l(F))/\tau_D(F)$. In [19] the model was developed assuming certain specific formulas for $R(F)$ and $\tau_D(F)$ based on experimental data for kinesin-1, while $v(F)$ was left as free. Here, in order to compare results with the MFM, we consider $v(F)$ as a known relation instead of $\tau_D(F)$. Then, the value of $\tau_D(F)$ entering in the algorithm is determined by inverting the corresponding formulas. For the $R(F)$ we consider the experimentally based [30, 31, 32] formula $R(F) = A \exp(-\log(A)|F|/F_s)$, with $A = 1000$ and F_s the before mentioned single motor stall force that leads to $P_r = P_l$. For the backward motors we consider the same single motor model but interchanging right and left. The forces f_i are computed assuming the cargo is linked to each motor by a non linear spring [8, 17] which produces

only attractive interactions, and only for distances larger than a critical one. Let us call x_i the position of motor i and $\Delta_i = x_i - x_c$. We define $f_i = k(\Delta_i - x_0)$ for $\Delta_i \geq x_0$, $f_i = 0$ for $-x_0 < \Delta_i < x_0$ and $f_i = k(\Delta_i + x_0)$ for $\Delta_i \leq -x_0$, with $x_0 = 110 \text{ nm}$ [8, 17]. Here, k is the stiffness of the motor for which we consider values k_f and k_b for forward and backward motors respectively. Note that while in [19] we have included volume excluded interaction between motors, here we consider only interactions mediated through cargo.

The detachment and attachment processes occur according to the probabilities per time unit indicated at the beginning of this section. The attachment of detached motors occurs with equal probability in any of the discrete sites x_j satisfying $|x_j - x_c| < x_0$.

2.3. Relevant quantities and numerical simulations

We study the cargo dynamics within MFM and SM by performing numerical simulations of the evolution of the system for different values of the parameters. As initial condition (at time $t_{ini} \equiv 0$) we consider a random number of motors of each species engaged on the microtubule. Each realization finishes when all the motors are detached (at time referred to as t_{end}). The numerical simulations of the SM are performed as explained in [19] using time steps between $dt = 2 \times 10^{-5} \text{ s}$ and $dt = 3 \times 10^{-7} \text{ s}$ depending on the value of γ . For the MFM we use our implementation of the Gillespie algorithm explained in [12, 28].

In order to characterize the long-time properties of cargo dynamics we compute the following quantities.

- *Cargo mean velocity.* Defined as the average over realizations of the ratio $(x_{end} - x_{ini}) / (t_{end} - t_{ini})$.
- *Run length.* Defined as the average over realizations of $(x_{end} - x_{ini})$.
- *Run time.* Denoted as τ_r , equal to the average of $(t_{end} - t_{ini})$.

Concerning the analysis of the dynamical properties during forward and backward stages of the motion, we compute the *mean forward run length* (r_f) and the *mean backward run length* (r_b). We define them as the average distance traveled by the cargo during the time intervals at which $n_f > n_b$ and $n_f < n_b$ respectively. Note that the association of forward (backward) motion of the cargo with $n_f > n_b$ ($n_f < n_b$) makes sense only for symmetric motors (i.e. equal parameters for motors of both polarities). For asymmetric motors, the characterization of forward and backward stages of motion demands a signal analysis of the trajectories including filtering and appropriate definitions of switching points and forward and backward runs, as it is usually done in experimental works [33, 34]. Such kind of studies is out of the scope of the present work.

Note that, for the MFM with symmetric motors, any definition of forward and backward run lengths based on signal analysis of trajectories would lead exactly to the same results as our definitions based on n_f and n_b . This is because, in such a case, the condition $n_f > n_b$ or $n_f < n_b$ determine the direction of motion. In contrast, within the SM, the exact coincidence between both kind of definitions cannot be ensured, since

for very short times we could have forward (backward) motion of cargo with $n_f < n_b$ ($n_b < n_f$). Nevertheless, the differences are expected to be small. In any case, the definitions in terms of n_f and n_b are relevant by themselves for our theoretical analysis.

3. Results for symmetric motors

First we analyze the results for both models considering equal parameters for forward and backward motors. For shortness, we speak of equal or symmetric motors. Except when specially stated, we consider single motor parameters compatible with kinesin-1 [12] for both models: $F_s = 6pN$, $v_0 = 1000nm/s$, $v_1 = 6nm/s$, $\epsilon = 1/s$, $F_d = 3.18pN$ and $\Pi_f = 5/s$. We left the numbers of motors N_f and N_b , and the viscosity as free parameters. For the SM, except when indicated, we consider the parameter $k = 0.32pN/nm$ usually taken as reference value for kinesin-1 [17].

3.1. Trajectories

As a first step in our study, we glance at the trajectories within both models. Figure 1.a shows cargo and motors trajectories for a system with $N_f = 2$ and $N_b = 1$ computed using the SM. Regions of tug of war leading to pauses and reversions of the cargo motion can be appreciated. In figure 1.b we show MFM and SM cargo trajectories for $N_f = N_b = 2$. At first glance we see that both models produce similar trajectories for such parameters. Thus, we can expect that this may lead to compatible results for ensemble averaged quantities. In contrast, results in figures 1.c and 1.d indicate us that, in the case $N_f = 3$, $N_b = 2$ both models predict very different results even at the level of single trajectories. Thus, depending on the parameters we may expect that the two models give results which may be statistically equivalent or not.

3.2. Results for negligible viscous drag

Now we begin our systematic analysis of both models focussing on the behavior of the cargo mean velocity, run length and run time. We analyze first the dynamics for negligible viscous drag. To do so, we consider the MFM without viscous drag [12], and the SM with a very small value of γ , so that the system is essentially at the zero viscosity limit. Actually, we use $\gamma = 9.42 \cdot 10^{-6} pNs/nm$, calculated using the Stokes formula [8, 17] with water viscosity and a radius of the cargo equal to $0.5\mu m$. Note that for such a value of γ , even if we consider a fast cargo velocity of $10^3 nm/s$ we get a viscous drag of order $10^{-2} pN$ which is quite small compared to the typical forces on the scale of $1pN$ involved in motor dynamics.

In figure 2 we study the case of a single species of motors considered with forward polarity. We plot the run length and the velocity as functions of the number of motors. The results are already well known from a number of previous works: the velocity is independent of the number of motors (for negligible viscosity), while the run length grows exponentially. Our contribution here is to show that both models agree in their

numerical results. As the analysis of single trajectories suggest and we will shortly confirm, this is not always the case when we consider two species of motors.

In figure 3.a we show results for the cargo velocity as a function of the number of backward motors N_b for fixed $N_f = 3$ in the symmetrical case. It can be seen that both models coincide only for $N_b = 0$ and $N_b = N_f$, while for intermediate values of N_b the MFM predicts considerably larger velocities. These differences are a consequence of the load sharing hypothesis. Note that, while in the MFM all engaged forward motors contributes equally to pulling the cargo, in the SM only those motors which are instantaneously beyond the limit distance x_0 from cargo exert non vanishing forces. Hence, each of such *pulling motors* are more loaded than motors in the MFM and, thus, their velocity is smaller. Clearly, this causes a smaller cargo velocity, since cargo velocity is essentially controlled by such leading motors. It is interesting to realize that for the SM we obtain the simple linear behavior $v = v_{0f}(N_f - N_b)/N_f$, regardless the value of the motor stiffness k . This demonstrates a certain degree of robustness of the motor team performance independently of the stalk stiffness. However, as we will see, other relevant quantities do depend on k . In figure 3.b we show the run time τ_r as a function of N_b for the same system as in figure 3.a. We see that, within the SM, τ_r increases with N_b and decreases with k . Except for vanishing N_b , the SM predicts sensibly larger values of τ_r than the MFM. Note that, while the cargo velocity is controlled by the pulling motors, the run time is expected to be essentially determined by the total number of engaged motors, regardless its polarity. This is because forward and backward motors contribute equally to linking the cargo to the microtubule (at least for symmetric motors). The relevance of differentiating between engaged and pulling motors was discussed in [19] when analyzing transport by a single species against an external load. The relation between run time and total number of engaged motors becomes evident with the results in figure 3.c, where we show the mean number of engaged motors as function of N_b for the same systems in 3.a and 3.b. The parallelism between curves in 3.b and 3.c is apparent. The total number of engaged motors increases with N_b , decreases when passing from MFM to SM and decreases with k within SM. The causes of these behaviours will be explained later when studying the probabilities of the different motility states. In figure 3.d we show the run length as a function of N_b for the same parameters as those in figure 3.a. and 3.b. As expected, the run length decreases with N_b in both models following the decrease of the mean velocity. Within the SM, the decrease of the run length with k can be associated to that of the run time and to the invariance of the mean velocity. This seems compatible with a factorization of the mean values. Interestingly, the results for the MFM are similar to those for the SM with $k = 0.32pN/nm$. However, this seems to be due to a compensation between the decrease of the velocity and the increase of τ_r when passing from the MFM to the SM.

Now we study the probabilities of the different states (n_f, n_b) for fixed N_f and N_b . This is relevant for finding out to what extent forward and backward motors coexist linked to the microtubule, and for evaluating the mean number of engaged motors. Let us take the case $N_f = 3$, $N_b = 1$ with $k = 0.32pN/nm$ as an example. Figures 4.a and

4.b show the probabilities of the different states (n_f, n_b) for SM and MFM respectively. Note that the state $n_f = n_b = 0$ has null probability as it determines the end of the simulation. The results clearly indicate that the states with one engaged backward motor are much more likely in the SM than in the MFM. Note that for the MFM, the states with $n_b = 0$ accumulate around a 85% of the probability. This means that the backward motor is detached most of the time. In particular, the states $(3, 0)$ and $(2, 0)$ alone dominate the dynamics a 80% of the time. In contrast, the SM predicts that the backward motor will be essentially half of the time engaged to the microtubule. Moreover the probabilities for the states $(3, 0)$, $(3, 1)$, $(2, 0)$ and $(2, 1)$ are all similar to each other. States with the backward motor engaged are more likely in the SM than in the MFM due to that, within the SM, the backward motor is unloaded a non negligible part of the time and, when it is loaded, it is in a tug of war only with those forward motors that are beyond the limit of $110nm$ from cargo. In contrast, in the MFM the engaged backward motor is all the time in a tug of war with N_f motors, each of which is less loaded than the backward motor. Within the SM, the probabilities of states with a backward motor engaged is found to decrease with the stiffness k , as we show in Figure 4.c. This is reasonable, since smaller stiffness lead to lower probability of detachment and results in more permissive of tug of war states. In the case of the system with $N_f = 3$ and $N_b = 2$ the results (not shown) are completely analogous to those for $N_f = 3$ and $N_b = 1$ in figure 4. Thus, we can state generally that the probabilities of states with engaged backward motors increase when passing from MFM to SM and, within the SM, they increase with decreasing k . This explains the increase of the mean number of engaged motors when changing from MFM to SM and when decreasing k (figure 3.c) as a consequence of the contribution of the tug of war states, which have larger total number of motors than single species states.

In figure 5 we show the results for r_f and r_b corresponding to the same systems analyzed in figure 3. As expected, r_f decreases monotonously with N_b in both models, since the probability of reversions grows with N_b . We also see that the SM predicts shorter forward excursions than the MFM. This is because the larger probability of having a backward motor engaged leads to a larger probability of changing from forward to backward motion. The results for r_b in figure 5.b are much more intriguing due to the abrupt variations with N_b . Nevertheless, we can give an almost complete explanation for them. Concerning the results for the SM, the counterintuitive fact that r_b is larger for $N_b = 1$ than for $N_b = 2$ is due to the contribution of the state $(n_f, n_b) = (1, 2)$ in the latter case. In fact, this state is found to be the one that largely contributes to r_b for $N_b = 2$ (it has probability $p = 0.096$ while states $(0, 2)$ and $(0, 1)$ have only $p = 0.035$ and $p = 0.017$ respectively). Clearly, the state $(1, 2)$ is expected to produce smaller velocities (and thus shorter runs) than state $(0, 1)$ which is the only one contributing to r_b for $N_b = 1$ (with $p = 0.019$). However, note that, for $N_b = 2$, the accumulated probability of having $n_f > n_b$ is larger than for $N_b = 1$. It thus happens that, for $N_b = 2$, backward excursions are shorter but more frequent than for $N_b = 1$. The results for r_b in the MFM are less intriguing, except maybe for the abrupt decrease when passing from

$N_b = 3$ to $N_b = 2$. This is simply related to that, due to equal force sharing, leaving the symmetric situation $N_b = N_f$ works largely against the species which results with lower number of motors.

3.3. Influence of the viscous drag

Now we analyze bidirectional transport under non negligible viscous drag. Figure 6.a shows the cargo mean velocity as a function of N_b for $N_f = 3$ considering a viscous drag equal to 1000 times that of water, both for MFM and SM. As expected, the velocities are smaller than those for water viscosity shown in figure 3.a (typically by a factor 1/2). The general behavior of both models is similar to that for water viscosity, with one relevant difference. Now, MFM and SM give different results even for $N_b = 0$. This is because, while in the MFM all the forward motors share the load coming from the viscous drag, in the SM the load acts essentially only on the pulling motors. The same would occur when considering any other kind of external load force acting against the advance of the cargo, as the results in [17] for a single motor species suggest. Figure 6.b shows the run times for the same systems analyzed in Figure 6.a. As in the case of the velocities, we find that the differences between both models extend to the case $N_b = 0$. Finally, we complete our analysis of the influence of viscous drag with the results in figure 6.c, which show the dependence of the cargo velocity on γ for systems with and without backward motors. It can be seen that, although the general dependence on γ for all systems and models are similar to each other (τ_r is constant for $\gamma \lesssim 5 \times 10^{-3} pNs/nm$ and decreases exponentially for $\gamma \gtrsim 5 \times 10^{-3} pNs/nm$), the predictions of both models coincide only in the case of low viscosity and no backward motors. Moreover, the differences between the results from both models increase with the addition of backward motors.

4. Results for uneven forward and backward motors

Now we leave the symmetric case and study the models considering backward motor parameters that can be associated to cytoplasmic dynein. For forward motors we continue using the kinesin-1 parameters considered in the previous section. Since the walking and detachment properties of dyneins are not as well known as for kinesin-1, the parameters for dyneins are not quite clear. Here we consider two different sets of parameter's values (named simply as set A and set B) based on the two proposals in [12, 13, 15]. Set A has been considered within MFM in [12] and with small changes in [15] on the base of previous experimental and theoretical results (see Table 1 in [12], supporting material in [15] and references therein). Set B was obtained by fitting experimental data on *Drosophila* lipid-droplet transport [12] and is consistent with previous experimental data [35]. According to set A, the main differences between dyneins and kinesin-1 appear in the binding and unbinding rates. In contrast, set B considers also important differences on the typical velocities and stall forces of both motor types. It is interesting thus to investigate the bidirectional motion of cargo

transported with kinesin-1 motors and both models of dyneins.

Note that for the SM, in addition to binding, unbinding and velocity parameters, it is also necessary to specify the forward-backward ratio of jumps as a function of the load force. Since we have not experimental data for dyneins, in this work we consider the same exponential form used for kinesins. The use of any other reasonable formula is not expected to produce relevant changes in the results. In fact in [19] it was shown that even the consideration of no backward steps produces relatively small changes for the case of transport by kinesins.

In figure 7 we show results for cargo transport by kinesins-1 and set A dyneins under negligible viscous drag. Since the differences between the parameters for both types of motors are relatively small, the results are similar to those for symmetrical motors. The effects of the asymmetry are mainly notable in the case $N_f = N_b = 3$, for which we observe a net backward motion. This can be seen both in the velocities in figure 7.a and in the trajectories in figure 7.b. The fact that set A dyneins win the tug of war for $N_f = N_b$ is mainly due to their slightly larger stall force. The differences between the predictions of MFM and SM for the velocities (figure 7.a) and the run times (figure 7.c) are considerably relevant, and they occur in a similar fashion to that observed for symmetrical motors. The same happens with the probabilities of having a backward motor engaged (figure 7.d), which are found to be larger for the SM than for the MFM. As in the case of symmetrical motors, this latter result helps us to understand the differences in the run times from both models. Going back to figure 7.b, we see that the SM trajectories are much more winding than those from MFM. This phenomenon is related to the reduction of r_f analyzed in the case of symmetric motors. The larger rate of reversion in the SM is due to that only some of the engaged motors pull the cargo at a given time and, in addition, it is more likely to have opposing motors engaged than in the MFM.

Now we consider dynein with parameter set B. In this case, dynein is a motor sensibly weaker than kinesin-1, since it has much lower stall force, much lower detachment force, lower attaching probability and also lower ratio F_s/F_d . Thus, for equal number of kinesin and dyneins, the kinesins win the tug of war. In fact, we find that several dyneins are needed to produce average null velocity for a cargo pulled by only one kinesin. In figure 8.a we show the cargo mean velocity as a function of N_b for systems with $N_f = 1$ and $N_f = 2$. It can be seen that for small N_b the velocity is similar for both models (almost coincident for the case $N_f = 1$). In contrast, for relatively large values of N_b the predictions of both models differ substantially. In particular, the number of dyneins needed to attain zero average velocity for a cargo pulled by one or two kinesins are considerably different. For $N_f = 1$ we find $N_b \sim 8$ for the MFM and $N_b \sim 12$ for SM, while for $N_f = 2$ we find respectively $N_b \sim 14$ and $N_b \sim 20$.

Figure 8.b shows the dependence of the run time on the number of dyneins for a cargo pulled by one kinesin. It can be seen that, even for $N_b < 4$ for which both models give similar mean velocities, they predict quite different results for τ_r . In the region $n_b \sim 8$, the situation is the opposite, both models give similar run times but they

predict quite different velocities. For $n_b > 8$ the run time in the MFM grows very fast with n_b due to that dyneins win the tug of war (the mean velocity is negative). This makes dyneins to remain mostly attached while the only kinesin detaches. Thus, the total number of engaged motors which controls the run time increases.

In figure 8.c we show results for the probabilities of the different states for a system with $N_f = 1$ and $N_b = 4$. For simplicity, we show only the probabilities of states with $n_f = 1$ (states with $n_f = 0$ have very small contributions in both models). Again, the SM gives a much larger probability of engagement of backward motors than the MFM.

Finally, we briefly explore the influence of the viscosity and of possible differences on the stiffness of motors from both species. In figure 8.d we study the effective number of set B dyneins needed to achieve zero mean velocity when pulling against one kinesin. We consider different values of γ and k_b . Note that our results provide non integer effective values for N_b which correspond to interpolations leading to zero cargo velocity. We see that for the MFM the results are almost independent of γ at a value close to $N_b = 8$. Interestingly, this value can be estimated by equating the powers produced by both motor teams considering all the motors attached at stall force. Namely, considering $N_b \times v_{sb} \times f_{sb} = v_{sf} \times f_{sf}$ we get to $N_b = 8.39$. The behavior within the SM is much more complex. The effective number of dyneins needed to stop a kinesin depends both on the viscosity and the stiffness. Actually, it decreases with γ and increases with k_b . The decrease with γ is clearly due to that viscosity helps to stop the cargo. The increase with k_b is due to that larger k_b lead to less force production by dyneins, due to easier detachment. Note that we have considered a quite small value for the dynein's stiffness ($k_b = 0.08 pN/nm$). The reason for this is twofold. First, it is the only way to reduce to reasonable values the effective number of set B dyneins needed to attain null velocity when pulling against one kinesin. Second, recent experiments [36] for transport mediated by dynein and kinesin-2 reported values of the stiffness in such range.

5. Conclusions

Cargo transport along microtubules mediated by two opposing motor species provides interesting challenges both from the experimental and theoretical points of view. With the main aim of understanding the consequences of specific modeling assumptions, in this paper we have theoretically analyzed several aspects of the problem considering two different mathematical models: the mean field model (MFM) [12], and a recently introduced stochastic model (SM) [19] which share some commons with models in [8] and [17]. The main difference between the MFM and the SM stems from the assumptions of force sharing by the different motors. The MFM assumes equal load sharing by all the engaged motors of the same polarity while SM considers individual cargo motor linking allowing for uneven force sharing.

Our main results indicate that both models show complete agreement only when there is essentially no load to share, that is, in systems with a single type of motors and with no relevant viscous effects. In other situations, the MFM predicts larger cargo mean

velocity and smaller mean run time than the SM. We have found that the differences in the velocities are mainly due to the fact that, within the SM (and in agreement with statements in [8, 17, 18]), only some of the engaged motors pull the cargo at a given time. Moreover, the probability of engaged backward motors during forward excursions is larger in the SM than in the MFM. This leads also to a larger rate of reversions within SM when compared with the MFM, or equivalently, to shorter excursions toward each polarity. The difference between the mean velocities predicted by both models is found to increase with the viscosity. We have also found that the mean run time is essentially controlled by the mean number of engaged motors at a given time, which depends on the probabilities of the different motility states and, ultimately, on the force sharing assumptions. Our results for the SM show that the mean cargo velocity turns out to be rather independent of the stiffness of the motor-cargo link (k). In contrast, the mean run time decreases with k approaching the MFM results for large k .

These conclusions were obtained analyzing ideal systems in which motors of opposite polarities have identical dynamical properties. In addition, in section 4 we have provided results for the asymmetric case of transport driven by kinesin-1 and cytoplasmic dyneins, considering two different sets of parameters for dyneins usually found in the literature.

Finally, it is interesting to mention the possibility of considering a hybrid-modeling framework taking advantage of the benefits of both kinds of models: the simplicity and computational advantage of the Gillespie formulation of the MFM, and the higher reliability of models including uneven force sharing. Note that the SM provides an alternative way to compute (numerically) the transition rates and velocities of the motility states entering in the Gillespie algorithm considering uneven load sharing. The same could be done with models such as those in references [8, 17]. Thus, when fitting the single motor parameters needed to reproduce experimental trajectories, different intermediate procedures combining computations with both kinds of models could be imagined, depending on the particular problem and on the a priori knowledge of the parameters.

Acknowledgments

SB acknowledge L. Bruno for useful discussions. Financial support from the Argentinean agencies CONICET (under Grant No. PIP 11220080100076) and CNEA, and from of the Spanish MICINN through project FIS2008-01240, co-financed by FEDER, are also acknowledged.

6. Figures

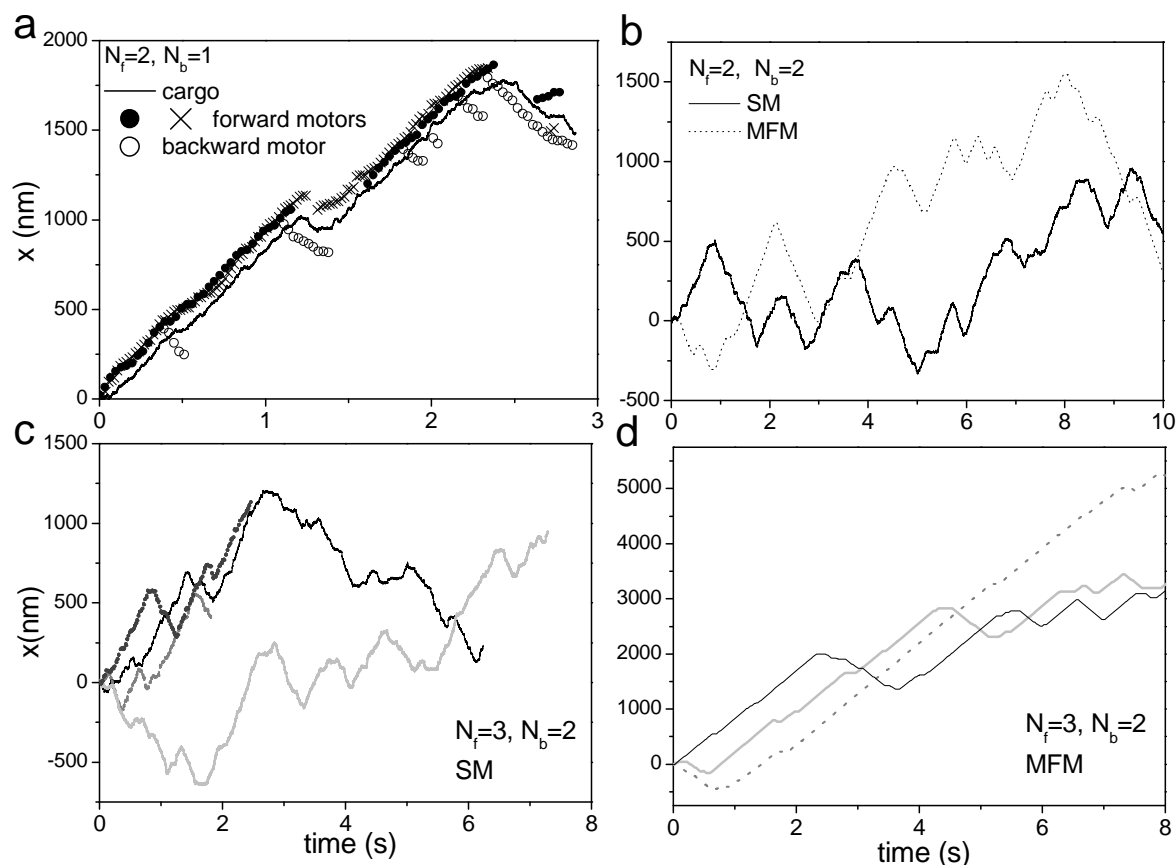


Figure 1. Trajectories. a) Typical cargo and motors trajectories for the SM considering $N_f = 2, N_b = 1$. b) Cargo trajectories for $N_f = N_b = 2$ for SM and MFM. c) Several different cargo trajectories for $N_f = 3$ and $N_b = 2$ for SM. d) Ibid c for MFM. In all the cases the viscosity considered is 100 times the water viscosity.

- [1] Howard J 2001 *Mechanics of Motor Proteins and the Cytoskeleton* (Sunderland, MA: Sinauer Associates).
- [2] Schliwa M and Woehlke G 2003 Molecular Motors *Nature* **422** 759-65.
- [3] L.S.B. Goldstein and Z. Yang. Microtubule-based transport systems in neurons: the roles of kinesins and dyneins. *Annu. Rev. Neurosci.* **23** 3971, 2000
- [4] Gross SP 2004 Hither and yon: a review of bi-directional microtubule-based transport. *Phys. Biol.* **1** R1-R11.
- [5] Welte MA 2004. Bidirectional Transport along Microtubules. *Current Biology* **14** R525 - R537.
- [6] Kolomeisky A B, Fisher M E 2007. Molecular Motors: A Theorist's Perspective, *Annu. Rev. Chem.* **58** 675-695.
- [7] Lipowsky R , Beeg J, Dimova R, Klumpp S, Muller MJI 2010 Cooperative behavior of molecular motors: cargo transport and traffic phenomena. *Physica E* **42** 649-661
- [8] Kunwar A, Vershinin M, Xu J, and Gross SP, 2008 Stepping, Strain Gating, and an Unexpected Force-Velocity Curve for Multiple-Motor-Based Transport *Current Biology* **18** 1173.
- [9] Korn CB, Klupp S, Lipowsky R and Scharz US, Stochastic simulations of cargo transport by processive molecular motors. *J. Chem. Phys.* **131**, 245107 (2009).
- [10] Shubeita GT, Tran SL, Xu J, Vershinin M, Cermelli S, Cotton SL, Welte MA, Gross SP 2008, Consequences of Motor Copy Number on the Intracellular Transport of Kinesin-1-Driven Lipid Droplets. *Cell* **135** 1098-1107.

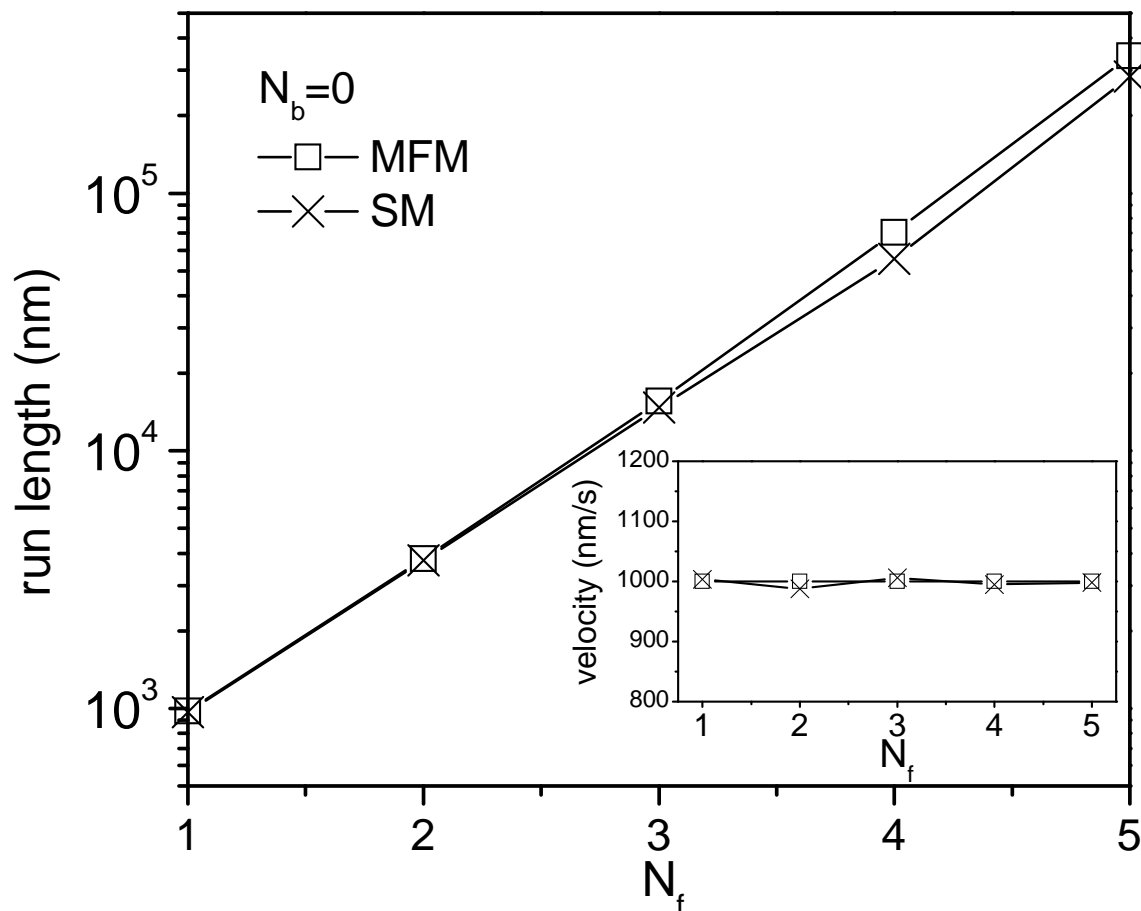


Figure 2. Results for a single team of motors ($N_b = 0$). Run length and cargo mean velocity (inset) as functions of N_f for SM and MFM considering water viscosity.

- [11] Klumpp S, Lipowsky R 2005 Cooperative cargo transport by several molecular motors. *Proc Natl Acad Sci USA* **102**, 17284-17289
- [12] Muller MJI, Klumpp S, Lipowski R 2008 Tug-of-war as cooperative mechanism for bidirectional cargo transport by molecular motors. *Proc Natl Acad Sci USA* **102**, 17284-17289
- [13] Melanie J.I. Muller, Stefan Klumpp, Reinhard Lipowsky (2008), Motility States of Molecular Motors Engaged in a Stochastic Tug-of-War, *J Stat Phys* 133: 1059-1081.
- [14] Zhang, Y (2009) Properties of tug-of-war model for cargo transport by molecular motors, *Phys. Rev. E* **79**, 061918
- [15] Muller MJI, Klumpp S, Lipowsky R, 2010 Bidirectional Transport by molecular motors: Enhanced Processivity and response to external forces. *Biophys. J.* **98** 2610-2618.
- [16] Erickson RP, Jia Z, Gross SP, Yu CC (2011) How Molecular Motors Are Arranged on a Cargo Is Important for Vesicular Transport. *PLoS Comput Biol* **7** (5): e1002032.
- [17] Kunwar A and Mogilner A, Robust transport by multiple motors with nonlinear force-velocity relations and stochastic load sharing. *Phys. Biol.* **7** (2010) 016012.
- [18] Jamison, DK, Driver, JW Rogers, AR, Constantinou, PE Diehl, MR. (2010) Two Kinesins Transport Cargo Primarily via the Action of One Motor: Implications for Intracellular Transport. *Biophysical Journal* **99** 2967-2977.
- [19] Bouzat S, Falo F 2010. The influence of direct motor-motor interaction in models for cargo transport by a single team of motors. *Phys.Biol.* **7** 046009.

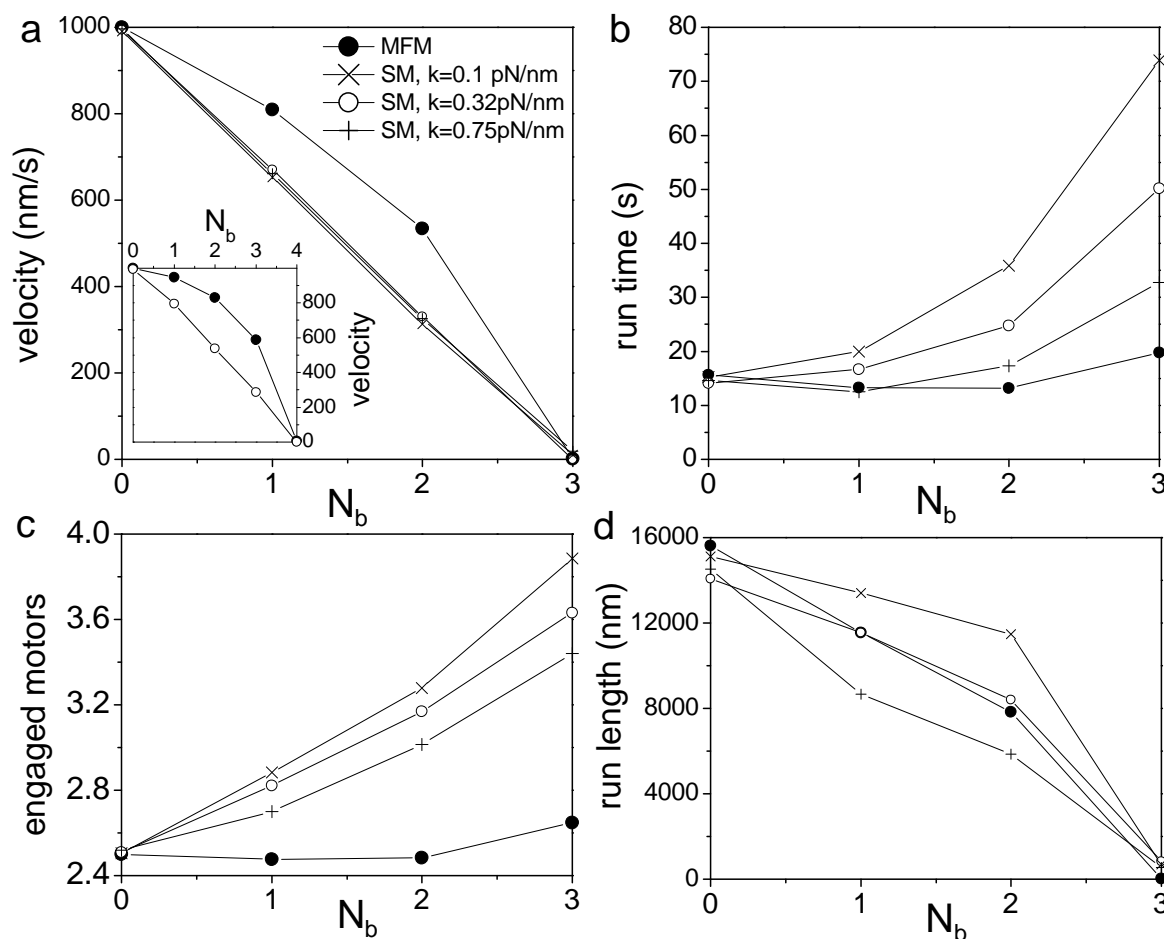


Figure 3. Cargo mean velocity (a), mean run time (b), mean number of engaged motors (c) and run length (d) as functions of N_b for systems with $N_f = 3$. Results for mean field and stochastic models under conditions of negligible viscous drag. In all the cases we consider kinesin-1 parameters both for forward and backward motors. The inset in panel (a) shows velocity results for $N_f = 4$ whose analogy with those for $N_f = 3$ indicates that the latter case (studied throughout the paper) is typical.

- [20] Zhang, Y (2011) Cargo transport by several motors, *Phys. Rev. E* **83** 011909
- [21] Campas O, Kafri Y, Zeldovich KB, Casademunt J, Joanny JF, 2006 Collective Dynamics of Interacting Molecular Motors *Phys. Rev. Lett.*, **97** 038101.
- [22] Brugués J, Casademunt J 2009 Self-Organization and Cooperativity of Weakly Coupled Molecular Motors under Unequal Loading *Phys. Rev. Lett.*, **102** 118104.
- [23] Hexner D, and Yariv Kafri Y, 2009. Tug of war in motility assay experiments *Phys. Biol.*, **6** 036016 (15pp).
- [24] Gur B. and Farago O 2010. Biased Transport of Elastic Cytoskeletal Filaments with Alternating Polarities by Molecular Motors *Phys. Rev. Lett.* **104**, 238101.
- [25] Gillo D, Gur B, Bernheim-Groswasser A and Farago O 2009 Cooperative molecular motors moving back and forth *Phys. Rev. E* **80** 021929.
- [26] Nedelec F 2002. Computer simulations reveal motor properties generating stable antiparallel microtubule interactions. *J. Cell Biol.* **158** 1005
- [27] Wollman R, Civelekoglu-Scholey G, Scholey J M and Mogilner A 2008. Reverse engineering of

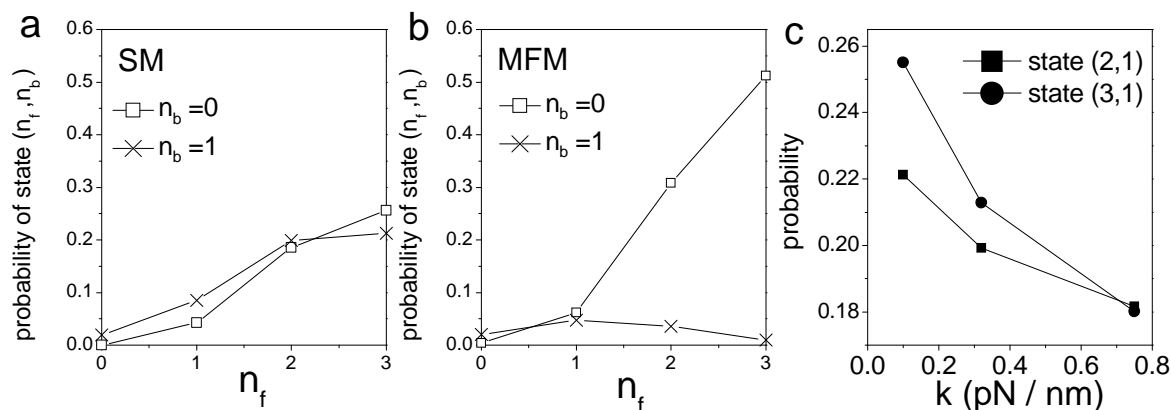


Figure 4. Probability of the states (n_f, n_b) for a system with $N_f = 3$ and $N_b = 1$ considering SM with $k = 0.32pN/nm$ (panel a) and MFM (panel b). Panel c shows the probabilities of the states (2, 1) and (3, 1) as functions of k within the SM. In all the cases, the normalization of the probabilities is such that their sum over the eight possible states is equal to one.

force integration during mitosis in the *Drosophila* embryo. *Mol. Syst. Biol.* **4** 195.

- [28] Gillespie DT, 1977. Exact stochastic simulation of coupled chemical reaction. *J. Phys. Chem.* **81**: 2340-2361
- [29] Van Kampen N G 1992, *Stochastic processes in physics and chemistry* (North-Holland. Elsevier Science Publishers B.V.)
- [30] Carter NJ and Cross RA 2005 Mechanics of the kinesin step *Nature*, **435** 308.
- [31] Schitzer MJ, Visscher K, Block SM 2000 Force production by single kinesin motors *Nature Cell Biology*, **2** 718-723
- [32] Hyeon C, Klumpp S, Onuchic JN 2009, Kinesin's backsteps under mechanical load, *Phys. Chem. Chem. Phys.*, **11**, 4899-4910.
- [33] Gross SP, Welte MA, Block S, Wieschaus EF 2000, Dynein-mediated Cargo Transport In Vivo: A Switch Controls Travel Distance. *The Journal of Cell Biology*, **148** 945.
- [34] Levi V, Serpinskaya AS, Gratton E, Gelfand V 2006, Organelle Transport along Microtubules in *Xenopus* Melanophores: Evidence for Cooperation between Multiple Motors, *Biphasical Journal* **90**, 318.
- [35] Mallik R, Petrov D, Lex SA, King SJ, Gross SP (2005) *Nature* 427:649652; King SJ, Schroer TA (2000) *Nat Cell Biol* 2:2024.
- [36] Bruno L, Salierno M, Wetzler DE, Desposito MA, Levi V (2011) Mechanical Properties of Organelles Driven by Microtubule-Dependent Molecular Motors in Living Cells. *PLoS ONE* 6(4): e18332

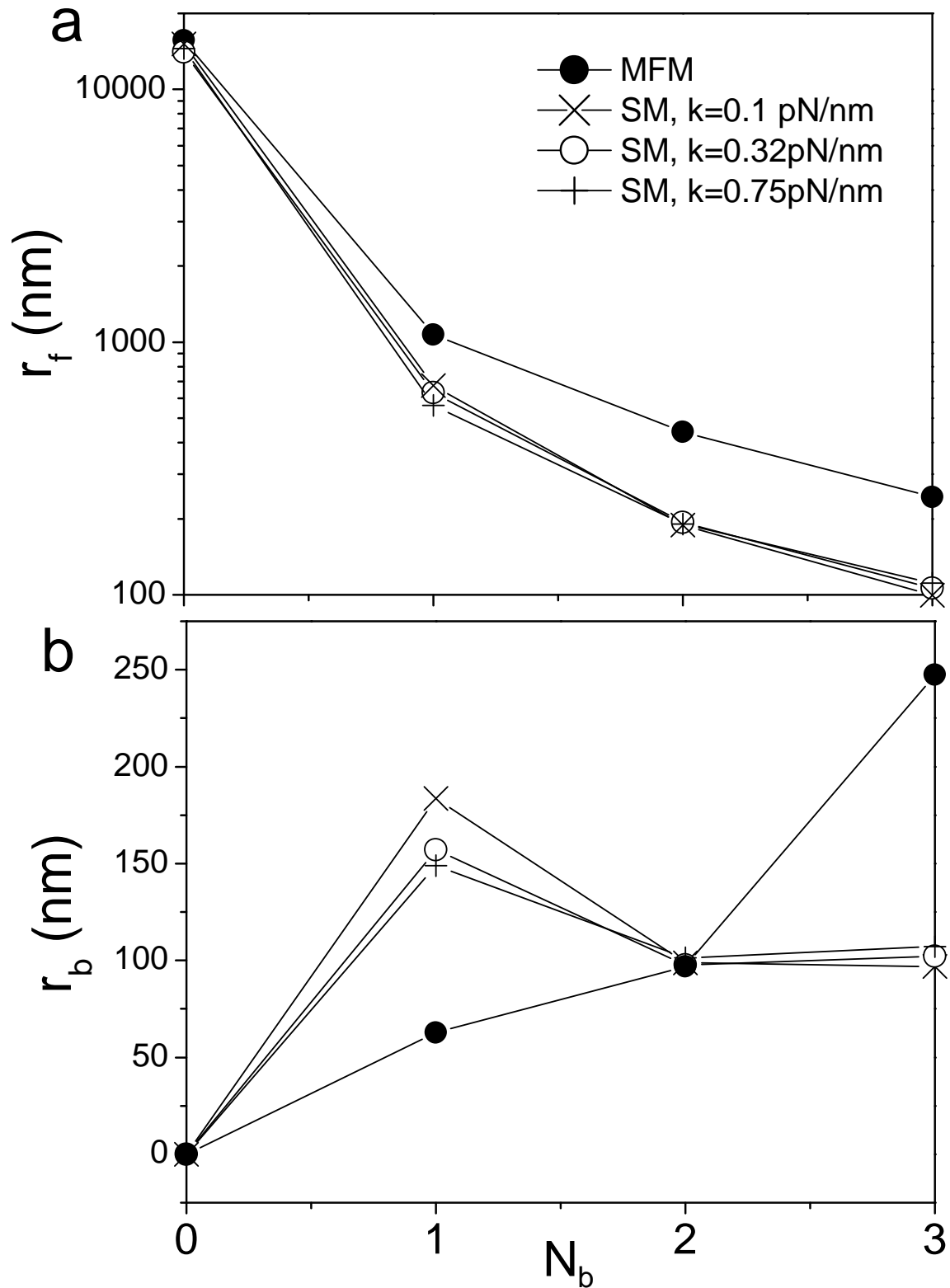


Figure 5. Results for r_f and r_b as functions of N_b for the same systems analyzed in figure 3, considering MFM and SM.

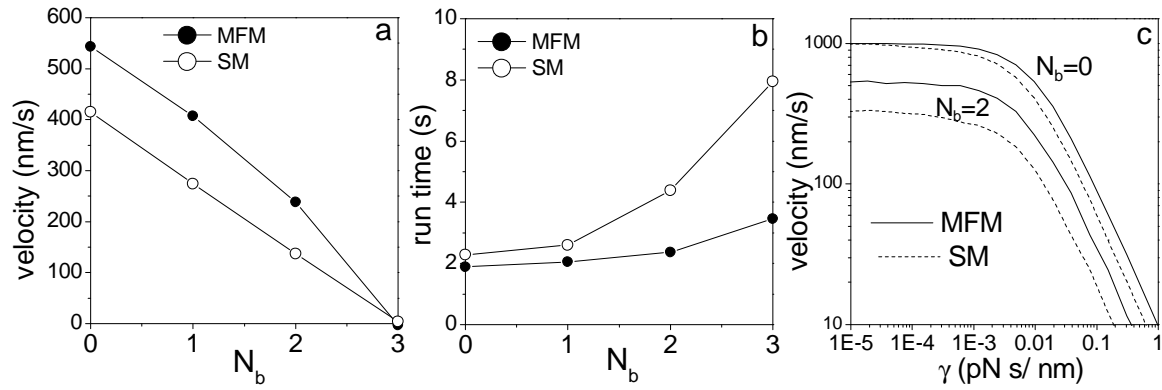


Figure 6. Influence of the viscous drag. Cargo mean velocity (a) and run time (b) as functions of N_b for fixed $N_f = 3$ considering $\gamma = 9.4210^{-3} pNs/nm$ for both models. This value of γ corresponds to a thousand times water viscosity and a cargo of 500 nm radio. c) Cargo mean velocity as a function of γ for $N_f = 3$ and different values of N_b for both models. All calculations within SM are for $k = 0.32 pN/nm$.

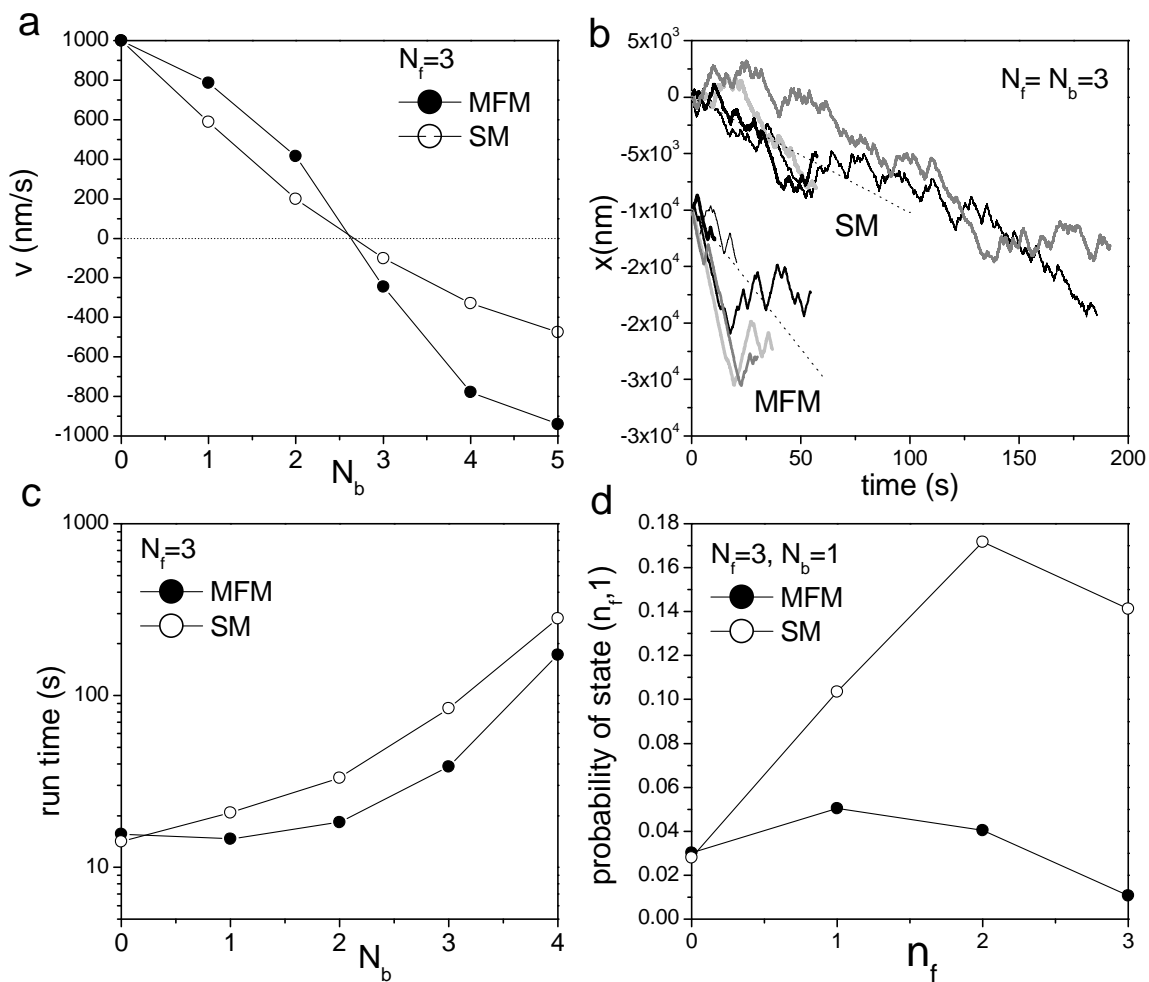


Figure 7. Kinesins and dyneins. Cargo mean velocity (a), cargo trajectories (b), mean run time (c) and probability of states with $n_b = 1$ (d) for a cargo pulled by kinesin-1 and dynein considering set A parameters for dyneins and negligible viscosity conditions for both models. Set A: $F_{sb} = 7.pN$, $Fdb = 3.18pN$, $\epsilon_b = 0.27s^{-1}$, $\Pi_b = 1.6s^{-1}$, $v_{0b} = 1000nm/s$ and $v_{1b} = 6nm/s$.

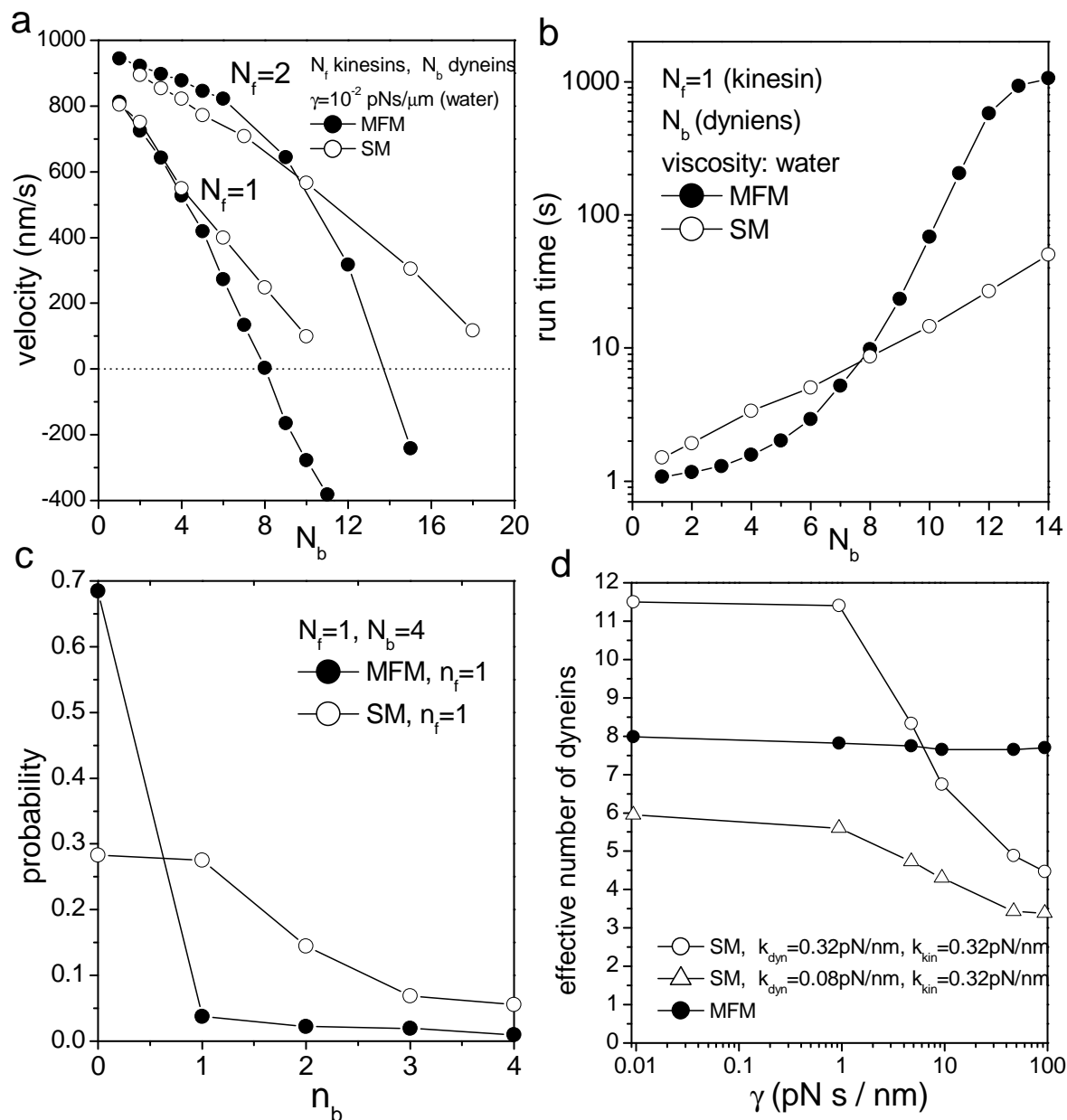


Figure 8. Kinesins and dyneins. Cargo mean velocity (a), mean run time (b) probability of different states (c) and effective number of dyneins leading to vanishing mean cargo velocity (d) for a cargo pulled by kinesin-1 and dynein considering set B parameters for dyneins and negligible viscosity conditions for both models. Set B: $F_{sb} = 1.1pN, F_{db} = 0.75pN, \epsilon_b = 0.27s^{-1}, \Pi_b = 1.6s^{-1}, v_{0b} = 650nm/s$ and $v_{1b} = 72nm/s$.